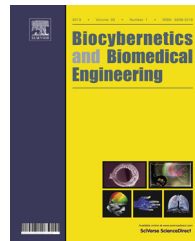


Available online at www.sciencedirect.com**ScienceDirect**journal homepage: www.elsevier.com/locate/bbe**Original Research Article****The ADHD effect on the actions obtained from the EEG signals****Reza Yaghoobi Karimui^{a,*}, Sasan Azadi^{b,*}, Parviz Keshavarzi^b**^a Faculty of New Sciences & Technologies, Semnan University, Semnan, Iran^b Department of Electrical Engineering, Semnan University, Semnan, Iran**ARTICLE INFO****Article history:**

Received 27 July 2017

Received in revised form

30 January 2018

Accepted 18 February 2018

Available online 2 March 2018

ABSTRACT

Attention-deficit/hyperactivity disorder (ADHD) is an important challenge in studies of children's ethology that unbalances the opposite behaviors for creating inattention along with or without hyperactivity. Nevertheless, most studies on the ADHD children, which employed the EEG signals for analyzing the ADHD influence on the brain activities, considered the EEG signals as a random or chaotic process without considering the role of these opposites in the brain activities. In this study, we considered the EEG signals as a biotic process according to these opposites and examined the ADHD effect on the brain activity by defining the dual sets of transitions between states in the complement plots of quantized EEG segments. The results of this study generally indicated that the complement plots of quantized EEG signal have a surprising regularity similar to the Mandala patterns compared to the chaotic processes. These results also indicated that the probability of occurrence of dual sets in the complement plots of ADHD children was averagely different ($p < 0.01$) from that of healthy children, so that the SVM classifier developed by these probabilities could significantly separate the ADHD from healthy children (99.37% and 98.25% for training and testing sets, respectively). Therefore, the complement plots of quantized EEG signals relevant to the ADHD children not only can quantify informational opposition caused by inattention, hyperactivity and impulsivity, but also these plots can provide remarkable information for developing new diagnostic and therapeutic techniques.

© 2018 Nalecz Institute of Biocybernetics and Biomedical Engineering of the Polish Academy of Sciences. Published by Elsevier B.V. All rights reserved.

Keywords:

ADHD

EEG

BIOS theory

Action

Complement plot

1. Introduction

Attention-deficit/hyperactivity disorder (ADHD) is a mental disorder of the neurodevelopmental type [1], which leads

to the lack of appropriate interaction with the environment [2]. Hence, the symptoms of this disorder are problems paying attention, excessive activity and difficulty controlling behavior [3,4], which usually reduce the children's performance for doing tasks. It is remarkable that 40–60% of children with this

* Corresponding authors at: Faculty of New Sciences & Technology, Semnan University, Semnan, Iran.

E-mail addresses: reza_yaghoobi@yahoo.ca, r_yaghoobi_k@semnan.ac.ir (R. Yaghoobi Karimui), sazadi@semnan.ac.ir, azadieng@yahoo.com (S. Azadi).

<https://doi.org/10.1016/j.bbe.2018.02.007>

0208-5216/© 2018 Nalecz Institute of Biocybernetics and Biomedical Engineering of the Polish Academy of Sciences. Published by Elsevier B.V. All rights reserved.

disorder can naturally reorganize their brain at over time for reducing these symptoms [5,6]. Nevertheless, the reduction of children's performance in the childhood due to the ADHD causes that the children do not get enough skill for the future [1]. Hence, the assessment of children in the childhood for the ADHD diagnosis is a great help to the children, parents, and especially the community health.

Currently, studies, which investigated the ADHD effects on the brain signals, can be generally considered as three groups. First group that examined the influence of ADHD symptoms on the event-related potentials (ERP) using continuous performance tests, and reported a different level of activity on the parietal and frontal lobes [7–9]. Second group that investigated the ADHD effects on the slow cortex potentials (SCP), and expressed that the contingent negative variations (CNV) in the ADHD children were lower than that of healthy children [10,11], and Last group in the data mining [12–14] and neurofeedback [15,16] that used the EEG signals. This group of studies, which employed the EEG frequency analysis for evaluating the ADHD effects on the standard EEG bands, revealed that the hyperactivity and impulsivity in the ADHD children increase the power of δ and θ bands and the inattention decreases the power of α and β bands. These studies in the biofeedback [15–19] also relied on a neurofeedback course for improving the ADHD symptoms, which indicates the self-organizing capability and the creativity of brain networks. Pharmaceutical studies on these children also portrayed a latency at the P200, N200 and P300 waves of event-related potentials [20], which displays the influence of misbehaviors internalized in these children on the attention (alerting, orienting and conflict [21,22]) and sensorimotor networks.

These finding in the behavioral indicators and the indicators obtained from the brain signals, therefore, not only confirm different energy exchanges between internal and external feedbacks in the brain of children with ADHD, but also they indicate that the brain is an open, creative and self-organizing system, which can change the energy exchanges of its feedbacks for amplifying or weakening the ADHD. These finding in the data mining studies also indicate an informational opposition in the influence of hyperactivity, impulsivity and attention on the EEG signals, in which increasing hyperactivity and impulsivity is equivalent to increasing the energy of low frequency components (δ and θ), and increasing attention is equivalent to increasing the energy of high frequency components (α and β).

This informational opposition in the EEG bands, which its origin according to the $1/f$ EEG frequency spectrum is the change of actions generated by the activity of brain opposites (inhibitory and excitatory postsynaptic terminals) [23], and also the brain creativity, actually represent that the electrical activities stored in the EEG signals are not random or chaotic processes, rather they are resulted from the activity of complementary opposites (excitatory and inhibitory feedbacks), which the brain as a biotic system usually internalizes them during its interaction with the environment. In other words, any change in the frequency content of EEG signals such as the transient states or the variations relevant to disorders and diseases is dependent on the regularity of actions generated by the activity of brain opposites. In this

regard, Sabelli and Kauffman [24–31], which used the complement plot generated by two orthogonal and opposite components (sine and cosine) to quantify the coexistence of opposites in the process equation, reported a surprising regularity in the complement plots of biotic processes obtained by this equation, which are completely dependent on the actions received from the bipolar and complementary feedback of this equation (i.e. $g \times \sin(x_n)$). These researchers in the complement plots obtained from the heartbeat intervals also portrayed regularity similar to the Mandala patterns [24,30–32], which are usually influenced the cardiac disorders and diseases. The complement plots obtained from the rounded EEG signals of children with autism spectrum disorder also indicated a different regularity compared to that of normal children [33], which its reason according to the concepts of bios theory is the change of actions generated by the complementary opposites in the brain [24].

Nevertheless, although this regularity in the complement plots of EEG signals confirms the biotic nature of brain activities, and also indicate that the EEG actions and the informational opposition lay in them are informative to quantify changes resulted from disorders and diseases, most studies on these plots only focused on the visual differences of complement plots, and have actually provided no approach to quantify the regularity of complement plots obtained from the signals. Therefore, the objective of present study is to provide a new approach to quantify the complement plot of EEG signals obtained from children with and without ADHD. The remainder of this paper is organized as follows: Section 2.1 presents data acquisition and noise removal processes. Section 2.2 shows that the EEG is a homeo-biotic process and that the biotic processes can be distinguished from chaotic processes by the complement plot. Section 2.3 quantifies the regularity of complement plot by using the dual sets of transitions occurred between the states of complement plot. Section 3 illustrates experimental results, and finally, Section 4 presents the discussion and conclusion.

2. Materials and methods

2.1. Subjects

In this study, we examined 40 children with age range 7–10 years, in which 20 children were with ADHD (50% are healthy). These children were distinguished by helping a professional psychiatrist and information gathered from the detailed history of past and current functioning, and also the Conner's parent rating scales [34]. Fig. 1 shows T scores of impulsive-hyperactive extracted from the Conner's parent rating scale for all of the children. As seen in this figure, the T scores of impulsive-hyperactive for healthy children were approximately lower than 50, while these scores for the ADHD children were higher than 50.

For each of the children, the EEG signals were recorded from the Fz, Cz, Pz, C3 and C4 positions on the scalp according to 10-20 international system and under eyes-open resting conditions at 250 s. Average of A1 and A2 electrodes was employed as reference value. These electroencephalograms were taken in a psychiatric clinic sponsored by the

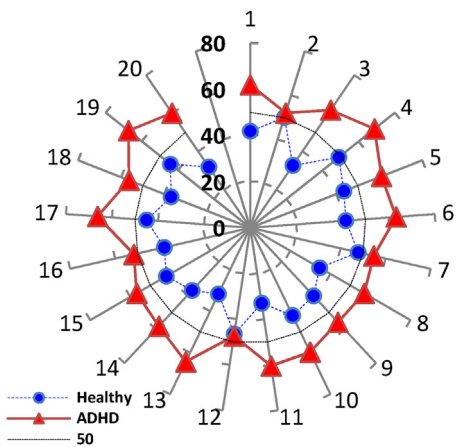


Fig. 1 – The T scores of impulsive-hyperactive extracted from the Conner's parent rating scales for all the children.

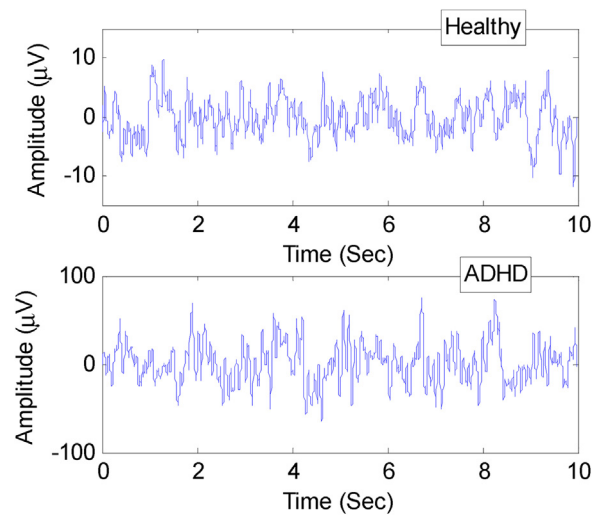


Fig. 2 – Samples of EEG signals taken from ADHD and healthy subjects.

Islamic Azad University (Mashhad in Iran) using a g.USBamp system.¹ The sampling rate of g.USBamp system was 256 Hz with resolution 24 bit. The band pass filter of this system was set to 0.1–100 Hz.

In the preprocessing phase, we first filtered signals by a Butterworth low pass filter (order 6) with 40 Hz cutoff frequency for removing high frequencies and power line noises. Then, we partitioned the EEG signals into segments of 10 s without overlap (the smallest frequency of EEG signals was 0.1 Hz) [2]. Fig. 2 shows the samples of EEG signals taken from ADHD and healthy children. In the next subsection, we illustrated that the EEG signal are a biotic process, and not a random or chaotic process.

2.2. EEG signal and biotic processes

The variations recorded on the EEG signal are resulted from the inhibitory and excitatory postsynaptic potentials [35] generated by the internal and external feedbacks, which have often the nonlinear, dynamic and casual behavior. Hence, the EEG generating system is a nonlinear dynamical system, which usually generates the transient states (local diversity) and the variations resulted from disorders and diseases (global diversity) due to its causality [24,27,30,31]. These properties, i.e. the causality coupled with the dynamicity and nonlinearity, in the EEG generating system have already caused that many researchers have considered the brain as a chaotic system [36,37]. Nevertheless, due to the random appearance of brain processes, these researchers have currently been forced to separately use two techniques: correlation dimension [38] and Lyapunov exponent [39,40] for justifying and proving the chaotic nature of brain processes.

In first techniques, i.e. correlation dimension, these researchers [38] usually used the growth trend of correlation dimension versus the changes of embedding dimension for separating the random from chaotic processes. Fig. 3 typically depicts the trends calculated for a set of random, chaotic,

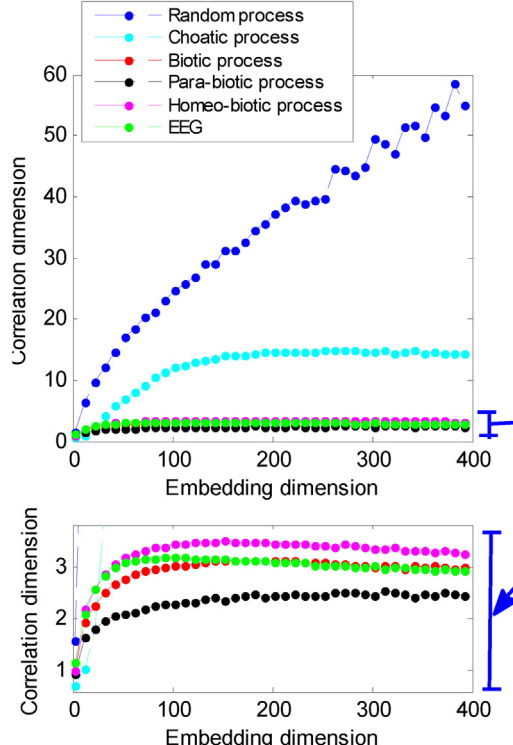


Fig. 3 – The relationship between correlation dimension and embedding dimension for the random, chaotic, biotic, para-biotic and homeo-biotic processes and the EEG signal.

biotic, para-biotic, homeo-biotic and brain (EEG) processes, which we generated them as following:

- **Chaotic process:** The chaotic process is one of the behaviors appeared in the states of nonlinear dynamic system, which is highly sensitive to initial conditions and has properties such as sustainability, repeatability and self-similarity

¹ Company site: <http://www.gtec.at/>.

[24,41]. This process, which exhibits a highly irregular behavior, is usually generated by strange attractors, which have very complex geometry. The logistic equation is one of the most common equations that can create these strange attractors [41]. Hence, we generated the chaotic process using this equation ($x_0 = 0.5$ and $g = 3.7$).

$$x_{n+1} = gx_n(1-x_n) \quad (1)$$

- **Biotic process:** The biotic process is another of the behaviors appeared in the states of nonlinear dynamic system, which has properties such as diversity, novelty, non-randomity, complexity and $1/f$ power spectrum in addition to highly sensitive to initial conditions. This process, which is apparently irregular, is usually generated by conserving the activity of feedbacks, which have the bipolar and complementary behavior. The process equation is one of the most common equations that can generate the biotic process in addition to chaotic process (this equation uses a sinusoidal term for generating the actions in its feedback) [24]. Therefore, we generated the biotic process using this equation.

$$x_{n+1} = x_n + g\sin(x_n) \quad (2)$$

- **Homeo-biotic process:** The homeo-biotic process is one type of the biotic processes, which its dynamic range is bounded. Cardiac patterns such as the heartbeat series are the natural examples of this type of processes. These bounded biotic series can be also constructed by adding the negative feedback to the action term in the process equation [24]. In the study, we employed following equation for generating the homeo-biotic process.

$$x_{n+1} = x_n + g\sin(x_n) - 0.01(x_n - 35\pi) \quad (3)$$

- **Para-biotic process:** the para-biotic process unlike the homeo-biotic process is an unbounded biotic process. Economic processes such as the daily Dow-Jones Industrial Average are the universal examples of this type of processes. The asymmetric process equation is one of the most common equations for generated the para-biotic processes. This equation is defined as following [24]:

$$x_{n+1} = x_n + g\sin(0.2 + x_n) \quad (4)$$

We used $x_0 = 0.5$ and $g = 31$ for generating the biotic processes.

- We also used an EEG segment selected from the healthy group (2560 sample recorded from Cz channel) and a Gaussian noise with zero mean and unit variance for the random and brain processes, respectively.

In total, as shown in the curves of this figure (Fig. 3), the growth trend of correlation dimension in the chaotic, biotic and brain (EEG) processes has a bound, while there is not such bound in that of random process. This difference in the trends thus indicates that the correlation dimension technique is only useful to distinguish the random from chaotic and biotic processes, and cannot clearly distinguish the chaotic from biotic processes. However, the biotic processes and the EEG signal had a smaller bound than the chaotic process.

In second techniques, i.e. the Lyapunov exponent, the researchers [39–41] usually employed the Lyapunov exponent

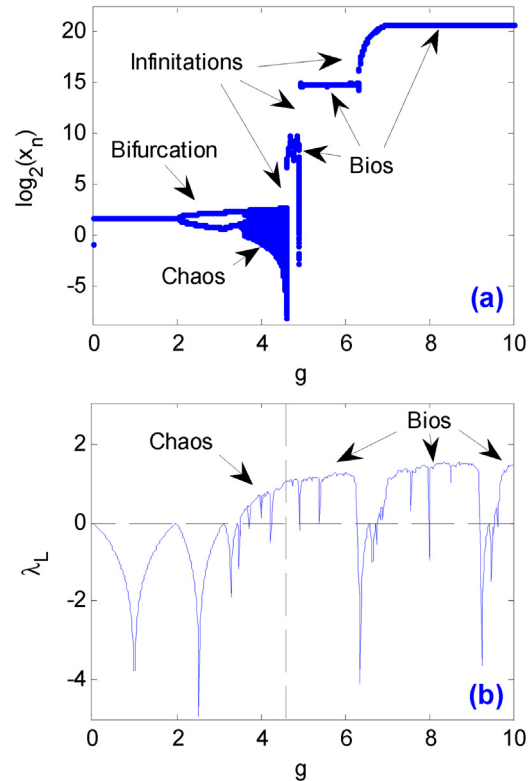


Fig. 4 – Bifurcation diagram (a) and Lyapunov exponent (b) for the process equation.

for identifying the chaotic behaviors in the equations and systems. In other words, these researchers considered a positive Lyapunov exponent equivalent to the chaotic behavior [39,41]. Although, this issue is acceptable in the chaotic systems, recent studies on the bios theory [24,25,27,30,31] demonstrate that the nonlinear dynamic systems can generate other behaviors (such as the biotic behavior), in which the Lyapunov exponent is a positive value. Fig. 4 typically indicates the bifurcation diagram and the Lyapunov exponent (λ_L) for the process equation. As shown in this figure, the Lyapunov exponent not only was a positive value for the chaotic series generated by the process equation, but also was also a positive value for the biotic series generated by this equation. This same condition in the chaotic and biotic processes generated by the process equation actually represented that the positive Lyapunov exponent is not a suitable indicator to distinguish the chaotic from biotic series. Therefore, a different technique is required to separate the chaotic from biotic processes.

The complement plot is one of the techniques introduced in the bios theory, which can be used to separate the chaotic from biotic processes [24–31]. According to Sabelli's studies [24], this plot using the sinusoidal forms (sine and cosine) decomposes a complex series into two orthogonal and opposite components. Therefore, if there is the organized opposite information in the actions of the complex series, this plot able to detect it.

Accordingly, in this work, we first normalized the processes between -1 and 1 . Then, we quantized the normalized processes in N levels and finally calculated the sine and

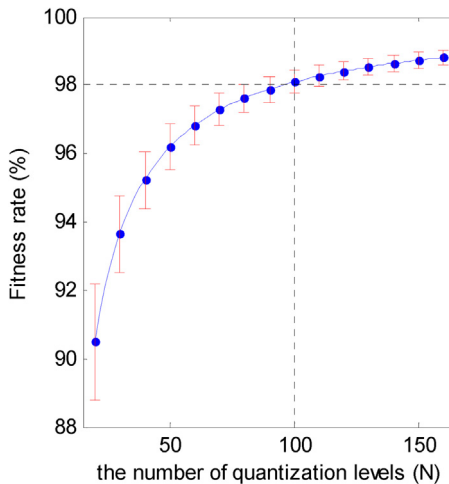


Fig. 5 – The effect of N parameter on the fitness rate of quantized EEG signal and the original EEG signal.

cosine of each term in the quantized process for drawing the complement plot. The following equation provides our method for the quantization.

$$x_q(n) = \text{round}\left(N\left[\frac{x(n)-x_{\min}}{x_{\max}-x_{\min}} - \frac{1}{2}\right]\right) \quad (5)$$

where x , x_q , x_{\min} , x_{\max} , N are the process, the quantized process, the minimum and maximum values of the x process, and the number of quantization levels, respectively. In this equation, the number of samples and the range of changes of the x_q process are dependent on the number of quantization levels (N). Therefore, this parameter has a decisive role in the structure (states and transitions) of complement plots.

Fig. 5 indicates the effect of this parameter (the N parameter) on the fitness rate of quantized and original EEG signals, according to 5000 EEG segments. As seen this figure, decreasing this parameter exponentially decreases the amount of information, which Eq. (5) carries from the original EEG signals to the quantized EEG signals. Therefore, a small N parameter cannot be suitable and the N parameter should be large enough. It is remarkable that a very large N parameter is not also true, because the information recorded on EEG signals has usually uncertainty due to environmental effects such as noise or technological error. Hence, in this research, we used $N = 100$ for drawing the complement plots of chaotic, biotic, para-biotic, homeo-biotic and brain (EEG) processes. This value only generates a fitness error about 2%, which is negligible.

Fig. 6 shows the complement plots obtained from the chaotic, biotic, para-biotic, homeo-biotic and brain processes, which we quantized them in 100 levels. Generally, as shown in these plots, the patterns of biotic, para-biotic, homeo-biotic and brain processes have only regularity geometry similar to the Mandala patterns, and the geometry of pattern relevant to the chaotic process completely is irregular. This regularity in the complement plots of biotic processes thus indicates that the complement plot is a suitable technique for separating the chaotic from biotic processes. The presence of this regularity in the complement plot of EEG signal also proves that the EEG

signal is a biotic process. In next subsection, we provided a method to quantify the transitions in the complement plot.

2.3. Quantify the regularity in complement plots

As shown in Fig. 6f, there is a set of concentric circles in the complement plot of quantized EEG signal, which has a special role in the regularity of patterns appeared in this plot. Nonetheless, these concentric circles have no the physical existence, and their main origin is the dual sets of transitions between the states in the complement plots, which is often created by changing the size and the occurrence time of its actions (i.e. $x_q(n+1) - x_q(n)$). Fig. 7a visually depicts these dual sets (DS_1-DS_5) for the complement plot obtained from an EEG segment quantized in 100 levels. As shown in Fig. 7b, the occurrence of each of these dual sets in a significant number of the states or all of the states can create one of the concentric circles marked in Fig. 6f. Therefore, we can investigate the regularity of complement plots in different diseases and disorders by using the probability (presence or absence) of each of these dual sets.

In this study, we estimated the probability of occurrence of each of these dual sets by using the following algorithm:

If x_q is an EEG segments quantized in the N levels.

1. Compute the sine and cosine of each term in the quantized EEG signal.

$$x_n = \sin(x_q(n)) \quad (6)$$

$$y_n = \cos(x_q(n)) \quad (7)$$

2. Calculate the Euclidean distance of each term from other terms as following:

$$d_n(i) = \sqrt{(x_n - x_i)^2 + (y_n - y_i)^2} \quad i = 1, 2, \dots, L \quad (8)$$

where L is the number of samples in an EEG segment.

3. Find points close to a state in the complement plot by using a small threshold defined on the Euclidean distance obtained in the previous step. This threshold can be equal to one-half of Euclidean distance between two states in the complement plot. We considered it equal to 0.05, which is approximately equal to one-fourth of the distance between two states in the complement plots provided in this research
4. Calculate angle between the x-axis and the vector created by each term (x, y) as following:

$$\theta_i = \begin{cases} \tan^{-1}\left(\frac{|y|}{x}\right) & x > 0 \& y > 0 \\ 2\pi - \tan^{-1}\left(\frac{|y|}{x}\right) & x > 0 \& y < 0 \\ \pi - \tan^{-1}\left(\frac{|y|}{x}\right) & x < 0 \& y > 0 \\ \pi + \tan^{-1}\left(\frac{|y|}{x}\right) & x < 0 \& y < 0 \end{cases} \quad (9)$$

5. Find the unique angles in the range of 0 to 2π ($\theta_1-\theta_{44}$ in Fig. 7a)
6. Find the dual sets marked in Fig. 7a using the angles (states) obtained in step 3
7. Calculate the frequency of each of the dual sets (n_j) in the quantized EEG segments

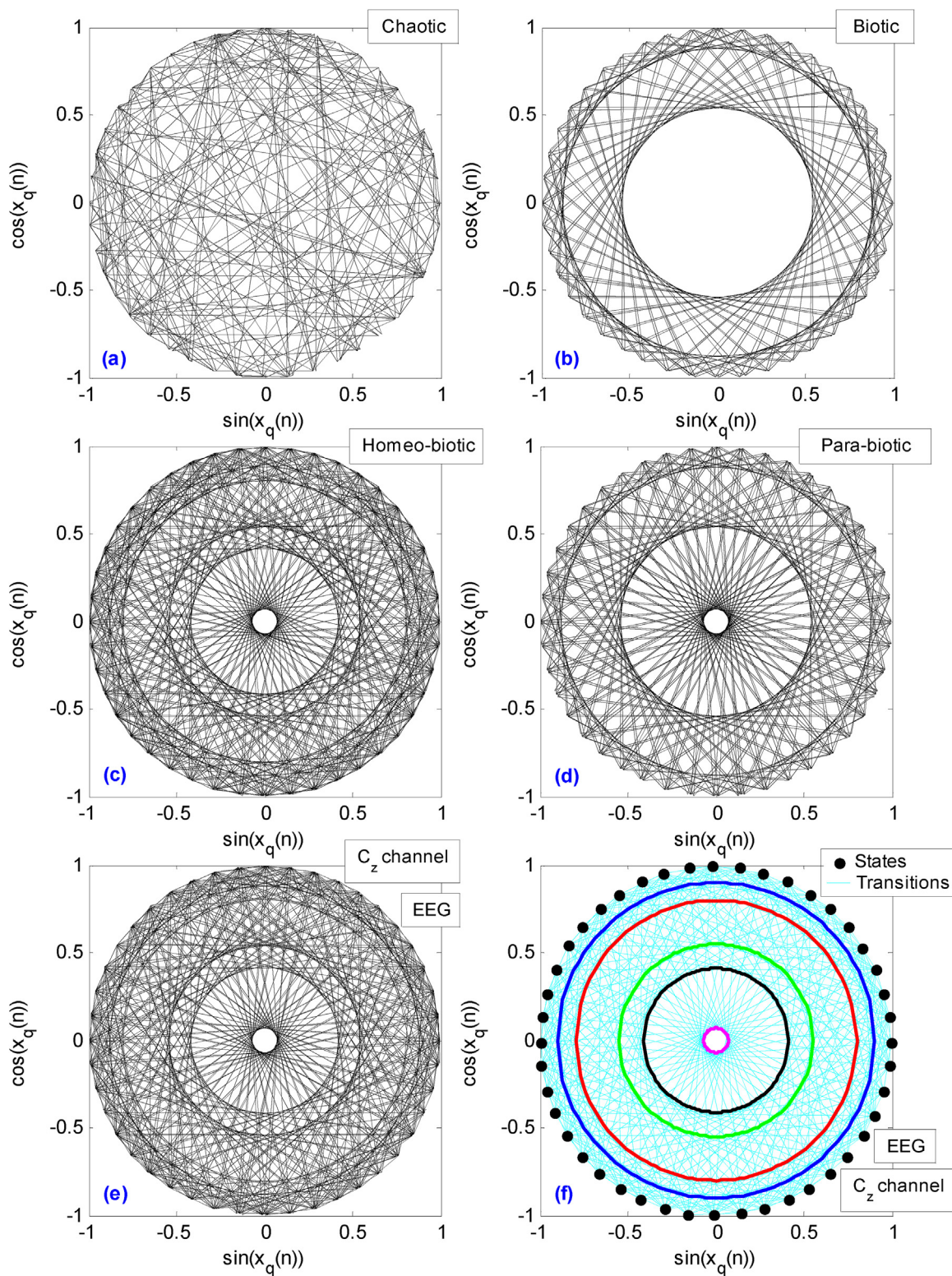


Fig. 6 – The complement plot: (a) the quantized chaotic process; (b) the quantized biotic process; (c) the quantized para-biotic process; (d) the quantized homeo-biotic process; (e) the quantized EEG signal; and (f) the concentric circles created by transitions between states in the complement plot of quantized EEG signal.

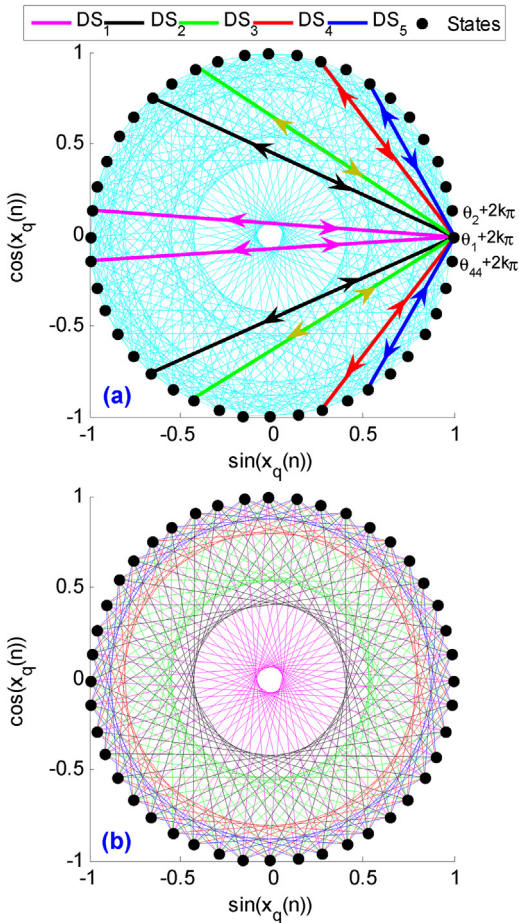


Fig. 7 – The diagrams show that: (a) the states (θ_1 – θ_{44}) and the dual sets of transitions between states (DS_1 – DS_5) for the complement plot of an EEG segment quantized in 100 levels; and (b) the effect of each of dual sets on the geometry of complement plot.

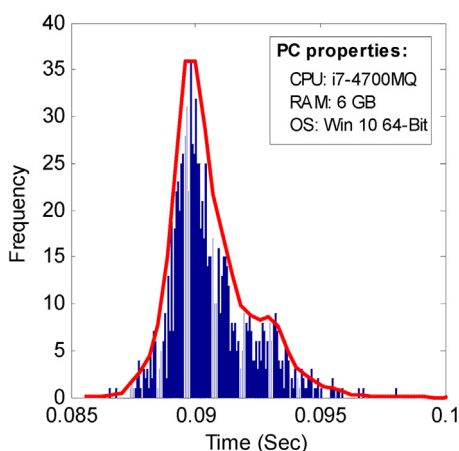


Fig. 8 – The time required to calculate the probability of the dual sets in 1000 EEG segments.

8. Calculate the probability of dual sets (DS_1 – DS_5) using the following equation:

$$p_j = \frac{n_j}{l-1}, \quad j = \{1, 2, 3, 4, 5\} \quad (10)$$

where l is the length of EEG segment. Evaluating the time required for computing the probability of occurrence of dual sets in a complement plot based on 1000 EEG segments is portrayed (Fig. 8). As seen this distribution, the proposed algorithm needs to a time between 0.085 s and 0.1 in each EEG segment. This time is almost equivalent to one hundredth of time required for recording an EEG segment used in the neurofeedback [42,43]. Therefore, this method can be used in pseudo-online applications such as the neurofeedback in addition to offline applications. In the next subsection, we examined the ADHD effects on the probability of occurrence of the dual sets.

3. Experimental results

As noted in the previous sections, the inhibitory and excitatory postsynaptic potentials generated by the internal and external feedbacks usually generate the variations of EEG signal. Therefore, the ADHD misbehaviors i.e. the hyperactivity, impulsivity and inattention are caused by the opposite activities (inhibitory and excitatory feedbacks), which the brain internalized them as a set of behaviors at over time. In other words, there is a relationship between the behaviors and the activity of brain opposites, which the ADHD uses it for changing the $1/f$ EEG frequency spectrum as the higher theta and delta bands, and the lower alpha and beta bands.

Fig. 9 typically depicts informational model, which we consider it for this relationship. As shown in this model, the ADHD misbehaviors are resulted from two behavioral opposites, which are psychologically opposed to each other. It is remarkable that the internalization effects of these behavioral opposites on the brain activities also lead to almost independent changes in the $1/f$ EEG frequency spectrum, which are opposed to each other. These opposites in the behavior and the brain activities thus cause that the brain of children with ADHD scrambles for stabilizing the attention, which its result is the irregularity of actions generated in the different levels of brain (compared to that of healthy children).

For displaying this irregularity in the brain actions recorded on the EEG signals, we according to the foundations of bios theory first considered the difference between two successive samples of quantized EEG segments as the action [24]. Then, we estimated the frequency distribution of actions in each of the quantized EEG signals, and finally calculated the variance of these frequency distributions in five EEG channels for the ADHD and healthy children. Fig. 10 shows these variances for the ADHD and healthy children. As seen in this figure, the pattern relevant to the EEG signals of ADHD children has relatively a greater variance in the larger EEG actions. This greater variance in the larger EEG actions of ADHD children, which its reason is the brain scramble for stabilizing the attention, actually represents that the ADHD shifts information from the smaller to larger EEG actions by creating the

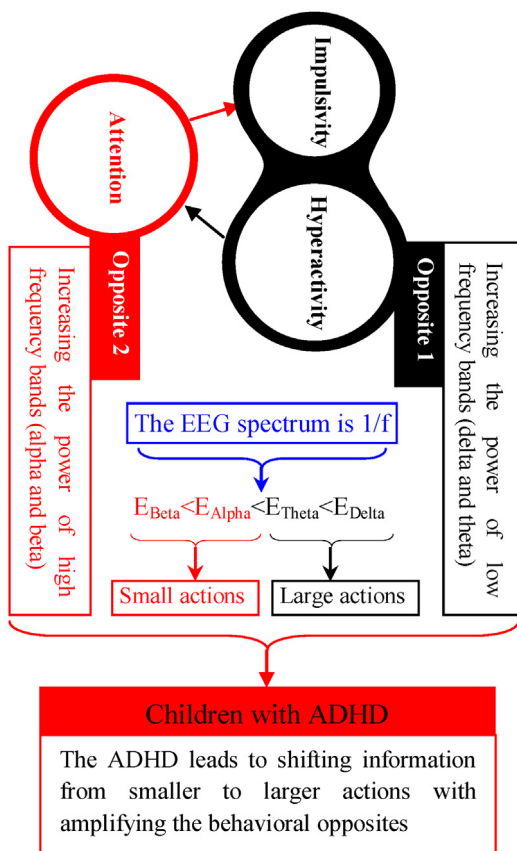


Fig. 9 – Informational model for describing the influence of two behavioral opposites resulted from hyperactivity, impulsivity and inattention on the brain activity of ADHD children.

irregularity in the brain actions. This shifting in the information thus cause that the complement plots obtained from the EEG signals of the ADHD children have averagely different regularity.

Fig. 11 typically shows the complement plot of two quantized EEG segment obtained from the ADHD and healthy children. As shown in the figure, the complement plot relevant to the ADHD children has visually a significant difference with that of healthy children, although this plot maintained the structure of complement plot relevant to the healthy children. This difference in the plots of Fig. 11 thus indicates that the transitions in the complement plots relevant to ADHD children have probably a different distribution compared to that of healthy children. Hence, we examined the probability of occurrence of the dual sets in the complement plot of EEG segments quantized in 100 levels for five EEG channels. Fig. 12 shows these probabilities for the ADHD and healthy children. Comparing these probabilities generally indicates a decrease in the probability of occurrence of dual sets 1–4 and an increase in the probability of occurrence of other transitions for the ADHD children, which means different distribution of transitions in the complement plots relevant to these children. accordingly, we considered the probability of occurrence of dual sets in an EEG segment obtained from five EEG channels

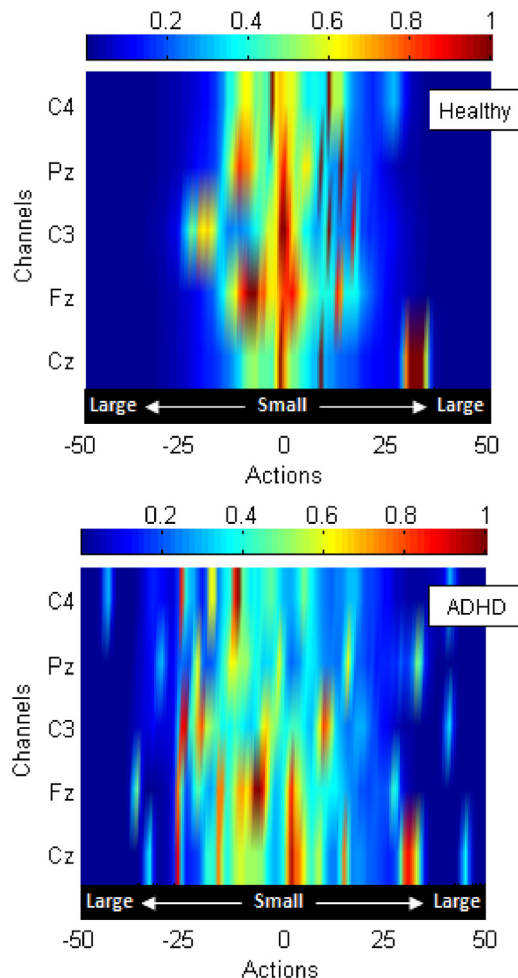


Fig. 10 – The variance of normalized frequency distributions obtained from the actions of quantized EEG segments in five channels.

as the feature and investigated these feature for the more accurate evaluation of the differences appeared in the complement plots relevant to the healthy and ADHD children.

Table 1 provides the *p*-values obtained from the paired-sample t-test analysis, and the accuracy of support vector machines (with the radial basis function (RBF) kernel and the scaling factor 1.35) for each of the features (the probability of dual sets) of whole dataset. As shown in this table, the *p*-values calculated for all of the features could reject the null hypothesis at the 1% significance level (*p* < 0.01). Similarly, the values of accuracy in this table confirm that the mentioned features could significantly distinguish the ADHD from healthy children. These results generally prove that the distribution of transitions between the states in the complement plots obtained from the EEG signals has notable information for separating the ADHD children. Of course, the t-test analysis can only examine the separation of features in one dimension. Hence, we used the following sequential forward selection (SFS) algorithm [44] for examining the separation of features in higher dimensions and selecting the optimal features.

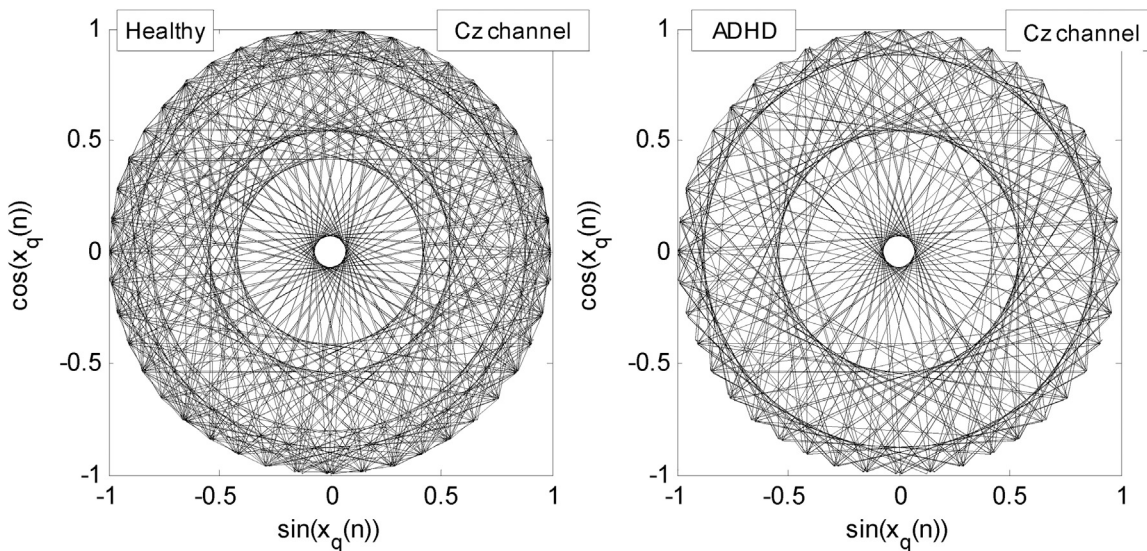


Fig. 11 – The complement plot of two quantized EEG segments obtained from the ADHD and healthy children.

SFS algorithm.

If $X = [x_1, x_2, \dots, x_N]$ is the input feature vector

1. Start with an empty set: $Y = []$
2. Select the next best feature using vector Y , $x_{\text{new}} \in X$ and the accuracy of RBF-SVM classifier
3. Go to 5, If the accuracy of selection criteria is larger than the previous step or desired accuracy. The selection criteria in this step was the accuracy of RBF-SVM classifiers developed by two training and testing sets obtained from the holdout method with the division rate of 40% for the testing set. The scaling factor of RBF kernel was also selected to the value of 1.35. This selection was according to the effect of scaling factor on the accuracy of RBF-SVM classifiers developed by the optimal features. Fig. 13 shows this effect. As shown in these curves, the selected scaling factor not only prevented from over training, but also this factor could create sufficient flexibility for the RBF kernel
4. Select Y for features. Go to 6
5. Replace x_{best} in Y and remove x_{best} in X . Go to 2
6. End

Fig. 14 provides the rank of features in the search trajectory of SFS algorithm established based on the accuracy of RBF-SVM classifier. These curves generally indicate that the combination of first 15 features could provide a significant accuracy for training and testing sets (99.35% and 98.60%, respectively). Comparing the results of 10-fold cross validation of RBF-SVM classifier developed by these features (optimal features) in Table 2 with the classification results reported in previous work (Table 3) also represented that the figure of merit (FOM) [2,44] for the RBF-SVM classifier developed by the 15 features was averagely 9.24%, and its maximum value was 27.46%.

$$\text{FOM} = \frac{98.25 - 98.07}{100 - 98.07} \times 100 = 9.24\% \quad (11)$$

$$\text{FOM}_{\max} = \frac{98.60 - 98.07}{100 - 98.07} \times 100 = 27.46\% \quad (12)$$

The optimal combination selected by the SFS algorithm also indicated that the Cz channel had a remarkable role in the search trajectory of SFS algorithm and all of the features (dual sets) extracted from this channel were the optimal selections for classifying the ADHD children. It is remarkable that the listed studies in Table 3 also confirmed that the Cz channel is informative. In the next section, we presented a brief discussion and conclusion about the results obtained in this study.

4. Discussion and conclusion

The EEG signals are resulted from opposite activities, which are largely generated by the cortical nerve cell inhibitory and excitatory postsynaptic terminals [35] fed by the different structural and functional levels such as the neural cells and networks. Therefore, the variations recorded on the EEG signals are dependent on the action of complementary opposites (inhibitory and excitatory synapses), which brain gradually adjusted them as a collection of agonist and antagonist components for creating its states and behaviors. In other words, these variations are a resultant of opposite information, which the brain usually generates them during the conservation and feedback of actions of its open, casual and opposite subsystems.

This condition in the EEG variations thus proves that the EEG signals have not the random or chaotic nature, rather a set of actions, which have regularity in the orthogonal and opposite spaces such as the complement plots due to their special internal opposition. In conforming this issue, the complement plots obtained from the rounded EEG signals of children with and without autism spectrum disorder in Sadeghi's report [33], and also the complement plots obtained from the quantized EEG signals of children with and without ADHD in this study have currently portrayed a regularity (non-randomness) geometry similar to the Mandala patterns, which

Table 1 – The p-value obtained from the t-test analysis for each of the dual sets (features), and the accuracy of RBF-SVM developed by each of the features.

Features	p-Value (t-test)	Accuracy
Dual set 4 (Cz channel)	1.11E–25	89.3
Dual set 1 (Cz channel)	1.90E–43	89.1
Dual set 2 (Cz channel)	3.25E–35	88.5
Dual set 5 (Cz channel)	4.14E–37	87.9
Dual set 3 (Cz channel)	3.54E–28	85.8
Other transition (Cz channel)	2.27E–30	85.8
Dual set 1 (Fz channel)	2.56E–24	85.5
Dual set 2 (Fz channel)	1.99E–19	83.9
Dual set 5 (Fz channel)	2.93E–21	83.8
Other transition (Fz channel)	7.97E–21	83.6
Dual set 4 (Pz channel)	3.90E–18	83.2
Dual set 3 (Fz channel)	7.42E–22	83.1
Dual set 5 (C3 channel)	3.88E–15	82.5
Dual set 2 (C3 channel)	7.03E–15	82.1
Dual set 4 (Fz channel)	9.12E–15	81.7
Dual set 1 (Pz channel)	8.74E–23	81.7
Dual set 2 (Pz channel)	9.39E–23	81.6
Dual set 4 (C4 channel)	5.99E–07	81.5
Dual set 3 (C3 channel)	1.49E–13	81.3
Other transition (C4 channel)	2.69E–08	81
Other transition (Pz channel)	1.53E–19	80.7
Dual set 1 (C3 channel)	7.68E–21	80.7
Dual set 5 (Pz channel)	7.17E–21	80.6
Dual set 4 (C3 channel)	1.55E–11	80.5
Other transition (C3 channel)	3.82E–16	79.9
Dual set 2 (C4 channel)	2.44E–09	79.7
Dual set 5 (C4 channel)	3.84E–09	79.6
Dual set 1 (C4 channel)	5.65E–13	79.5
Dual set 3 (Pz channel)	2.90E–18	79.4
Dual set 3 (C4 channel)	3.64E–10	78

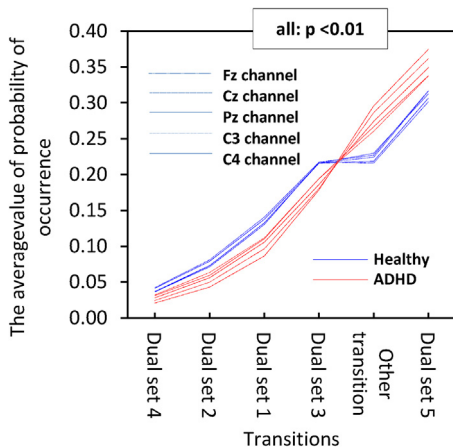


Fig. 12 – The probability of occurrence of each of the dual sets in the complement plot of EEG segments quantized in 100 levels.

represents the discipline of activities of brain subsystems in addition to proving the organized opposite content in the EEG actions. These plots in these disorders have also depicted diversity and novelty in the EEG signals (new regular pattern in the complement plots), which represents the creativity of

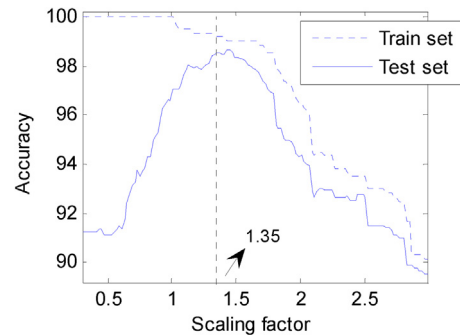


Fig. 13 – The effect of scaling factor on the accuracy of RBF-SVM classifiers developed by the optimal features obtained from the SFS algorithm.

nervous system for creating the destructive or evolutionary trends in the brain.

These properties, i.e. the nonlinearity, causality, non-randomness, opposition, diversity and novelty, in the EEG signals, therefore, not only prove that the EEG signal is a biotic process, but also indicate that the ADHD as a destructive factor is diversity and novelty in the human's behaviors, which brain creates it by changing its actions at over time. In other words, the gradual change of brain actions causes that children with ADHD often experience inattention and distractibility along with hyperactivity and impulsivity, which one of its results is the change of 1/f frequency content of brain activities recorded on the EEG signals as the higher theta and delta bands, and the lower alpha and beta bands [2,12–16]. It is remarkable that these changes in the EEG bands of ADHD children according to the finding of cognitive studies, which respectively reported the general arousal, attention and hyperactivity along with the decrease in the low-frequency power [61,62], the increase in the power of beta band [62,63] and the decrease in the power of theta band [64–66], indicate that the ADHD misbehaviors are resulted from two behavioral opposites (Fig. 9) internalized in the brain, which have a decisive role in the brain activities of ADHD children and the energy exchanges of these children with the environment due to the openness of nervous system and the 1/f EEG spectrum.

These opposites in the human's behaviors actually lead to a scramble in the brain of ADHD children for stabilizing the attention, which its result is the change of 1/f EEG frequency content as the higher theta and delta bands, and the lower alpha and beta bands, or in other words, the shift of information from the smaller to larger actions in the EEG signals (Fig. 10). The frequency distribution obtained from the EEG actions of children with and without ADHD by displaying an increase in the variance of distribution of EEG actions relevant to the ADHD children currently confirms this shift in the information. The probability of different occurrence in the transitions (dual sets) between the states of complement plots relevant to the ADHD children (Fig. 12) and the significant difference in these probability in five EEG channels for these children (Table 1) are also other confirmations for this shift in the information. The classification of these children using the

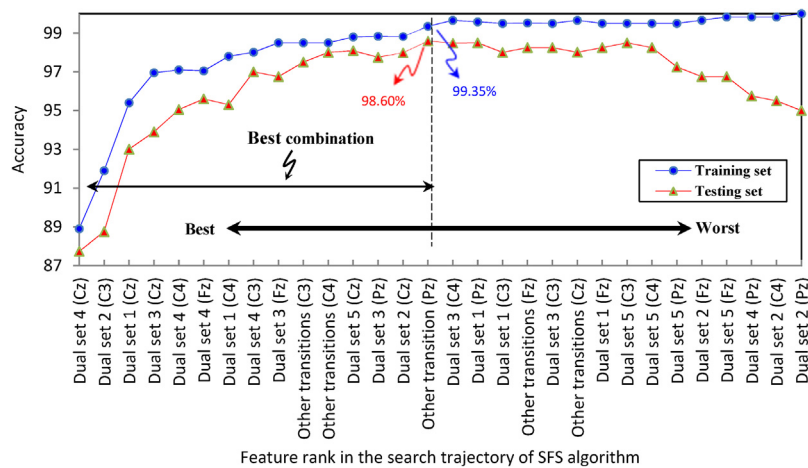


Fig. 14 – The output of SFS algorithm for classifying the children with and without ADHD.

Table 2 – The 10-fold cross validation of RBF-SVM classifier developed by the optimal features.

Classifier	Sets	Accuracy (%)		
		Max	Mean	Min
RBF-SVM	Train test	99.07 97.80	99.37 98.25	99.73 98.60

Table 3 – EEG-based studies for diagnosing the ADHD.

Author	Year	Number subjects	Age	Measures	Accuracy (%)
Nazari [9,45]	2011	16 ADHD and 16 control	7–13	Multi-channels, θ/β ratio	($p < 0.05$)
Williams [45,46]	2010	169 ADHD and 167 control	7–19	Fz/FCz, θ/β ratio	($p < 0.05$)
Loo [45,47]	2013	390 ADHD and 100 control		Cz, θ/β ratio	38
Liechti [45,48]	2013	54 ADHD and 51 control	8–16	Cz, θ/β ratio	53
Buyck [45,49]	2014	62 ADHD and 55 control	5–15 & 20–50	Cz, θ/β ratio	49–55
Helgadóttir [50]	2015	90 ADHD and 90 control	6.5–8.2	Multi-channels, optimal features extracted from the EEG band	79
		90 ADHD and 90 control	8.4–9.8		65
		90 ADHD and 90 control	10.4–12		78
		45 ADHD and 45 control	12.2–14		82
		315 ADHD and 315 control	6.5–14		76
Tenev [51]	2013	67 ADHD and 50 control	18–50	Multi-channels, absolute power ($\delta\theta\alpha\beta\gamma$)	82.3
Ogrim [45,52]	2012	62 ADHD and 36 control	7–16	Cz, absolute θ and β power θ/β ratio	85
Sadatnezhad [45,53]	2011	21 ADHD and 22 BMD	10–22	Multi-channels, Fractal dimension, AR model, band power ($\delta\theta\alpha\beta\gamma$)	86.4
Magee [45,54]	2005	75 ADHD and 75 control	7–13	Absolute and relative power	87
Ahmadiou [45,55]	2010	12 ADHD and 12 control		Inter-electrode synchronization ($\delta\theta\alpha\beta\gamma$)	87.5
Simoska [56]	2016	30 ADHD and 30 control	6–14	Cz, θ/β ratio	87.9
Snyder [45,57]	2008	97 ADHD and 62 control	6–18	Cz, θ/β ratio	89
Monastra [45,58]	2001	96 ADHD and 33 control	6–20	Cz, θ/β ratio	91
Mohammadi [59]	2016	30 ADHD and 30 control	7–14	Multi-channels, nonlinear optimal features	93.65
Abibullaev [45,60]	2012	7 ADHD and 3 control	7–12	Multi-channels, relative θ and β power, δ/θ and θ/α ratios	97
Yaghoobi [2]	2017	20 ADHD and 20 control	7–10	Continuous Wavelet Transform (CWT) and standalone classifier	98.07
This work		20 ADHD and 20 control	7–10	Complement plots	98.25

Note: The highest accuracy provided in previous work was 98.07%.

RBF-SVM classifier developed by these probabilities also provided a significant accuracy (99.37% and 98.25 for training and testing sets, respectively), which represents the remarkable shift of information from the smaller to larger actions.

In summary, although these findings have indicated that the EEG actions (or transitions between states in the complement plot) are informative to evaluate and maybe separate the ADHD from healthy children, these findings do not confirm that

we can completely separate the ADHD from healthy children, and actually the discriminators, which their diagnosis is based on an EEG segment, have often an error due to the overlapping of classes (ADHD and healthy). It is remarkable that researchers based on the concepts of pattern recognition currently know this error caused by the bad sampling, while the origin of this error is the creativity of brain. In other words, the accurate diagnosis of ADHD is impossible using an EEG segment due to the brain creativity, because this creativity can locate the children with and without ADHD in the same condition, which its result is the overlapping of brain activities in two groups. Therefore, it seems that subsequent studies must consider this issue to ensure a fuller investigation and provide more information about the repeatability and reliability of ADHD diagnosis using an EEG segment. Furthermore, since, the method proposed in this research have the capacity to use in pseudo-online applications, the comparison of mentioned reliability with the reliability of self-reports and the development of application based on the actions of EEG for the neurofeedback can be interesting start points for the future works.

REFERENCE

- [1] American Psychiatric Association. Diagnostic and Statistical Manual of Mental Disorders, Fourth Edition: DSM-IV-TR®. American Psychiatric Association; 2000.
- [2] Yaghoobi Karimu R, Azadi S. Diagnosing the ADHD using a mixture of expert fuzzy models. *Int J Fuzzy Syst* 2017;1:1–15.
- [3] Clauss-Ehlers CS. Encyclopedia of cross-cultural school psychology. Springer US; 2010.
- [4] Sroubek A, Kelly M, Li X. Inattentiveness in attention-deficit/hyperactivity disorder. *Neurosci Bull* 2013;29(1):103–10.
- [5] Pattanashetti N, Patil N, Tekkalaki B. Prevalence of adult attention deficit hyperactivity disorder in patients with bipolar affective disorder: a 1-year hospital-based cross-sectional study. *Indian J Health Sci Biomed Res (KLEU)* 2016;9(3):288–96.
- [6] Weiss M, Murray C. Assessment and management of attention-deficit hyperactivity disorder in adults. *Can Med Assoc J* 2003;168(6):715–22.
- [7] Silvana M-S, Nada P-J. Quantitative EEG in children and adults with attention deficit hyperactivity disorder. *Clin EEG Neurosci* 2016;48(1):20–32.
- [8] Poil SS, Bollmann S, Ghisleni C, OGorman RL, Klaver P, Ball J, et al. Age dependent electroencephalographic changes in attention-deficit/hyperactivity disorder (ADHD). *Clin Neurophysiol* 2014;125(8):1626–38.
- [9] Nazari MA, Wallois F, Aarabi A, Berquin P. Dynamic changes in quantitative electroencephalogram during continuous performance test in children with attention-deficit/hyperactivity disorder. *Int J Psychophysiol* 2011;81(3):230–6.
- [10] Gani C. Long term effects after feedback of slow cortical potentials and of Theta/Beta – amplitudes in children with Attention Deficit Hyperactivity Disorder (ADHD). *Int J Bioelectromagn* 2008;10(4):209–32.
- [11] Doehnert M, Brandeis D, Straub M, Steinhausen HC, Drechsler R. Slow cortical potential neurofeedback in attention deficit hyperactivity disorder: is there neurophysiological evidence for specific effects? *J Neural Transm* 2008;115(10):1445–56.
- [12] Clarke AR, Robert B, Rory MC, Mark S. Electroencephalogram differences in two subtypes of attention-deficit/hyperactivity disorder. *Psychophysiology* 2001;38(2):212–21.
- [13] Barry RJ, Clarke AR, Johnstone SJ. A review of electrophysiology in attention-deficit/hyperactivity disorder: I. Qualitative and quantitative electroencephalography. *Clin Neurophysiol* 2003;114(2):171–83.
- [14] Arns M, Heinrich H, Strehl U. Evaluation of neurofeedback in ADHD: the long and winding road. *Biol Psychol* 2014;95:108–15.
- [15] Pop-Jordanova N, Markovska-Simoska S, Zorsec T. Neurofeedback treatment of children with attention deficit hyperactivity disorder. *Prilozi* 2005;26(1):71–80.
- [16] Holtmann M, Sonuga-Barke E, Cortese S, Brandeis D. Neurofeedback for ADHD: a review of current evidence. *Child Adolesc Psychiatr Clin N Am* 2014;23(4):789–806.
- [17] Janssen TWP, Bink M, Weeda WD, Gelade K, Mourik RV, Maras A, et al. Learning curves of theta/beta neurofeedback in children with ADHD. *Eur Child Adolesc Psychiatry* 2017;26(5):573–82.
- [18] Leins U, Goth G, Hinterberger T, Klinger C, Rumpf N, Strehl U. Neurofeedback for children with ADHD: a comparison of SCP and theta/beta protocols. *Appl Psychophysiol Biofeedback* 2007;32(2):73–88.
- [19] Levesque J, Beauregard M, Mensour B. Effect of neurofeedback training on the neural substrates of selective attention in children with attention-deficit/hyperactivity disorder: a functional magnetic resonance imaging study. *Neurosci Lett* 2006;394(3):216–21.
- [20] Sunohara GA, Malone MA, Rovet J, Humphries T, Roberts W, Taylor MJ. Effect of methylphenidate on attention in children with attention deficit hyperactivity disorder (ADHD): ERP evidence. *Neuropsychopharmacology* 1999;21(2):218–28.
- [21] Fan J, McCandliss BD, Fossella J, Flombaum JI, Posner MI. The activation of attentional networks. *Neuroimage* 2005;26(2):471–9.
- [22] Raz A. Anatomy of attentional networks. *Anatom Rec B: New Anat* 2004;281B(1):21–36.
- [23] Yaghoobi R, Azadi S. Lossless EEG compression using the DCT and the Huffman coding. *J Sci Ind Res (JSIR)* 2016;75(10):615–20.
- [24] Sabelli HC. Bios: a study of creation. World Scientific; 2005.
- [25] Sabelli H, Novelty A. Measure of creative organization in natural and mathematical time series. *Nonlinear Dyn Psychol Life Sci* 2001;5(2):89–113.
- [26] Sabelli H. Arrangement, a measure of nonrandom complexity. *Syst Anal Model Simul* 2002;42(3):395–403.
- [27] Sabelli H. Complement plots: analyzing opposites reveals Mandala-like patterns in human heart beats. *Int J Gener Syst* 2000;29(5):799–830.
- [28] Sabelli H, Abouzeid A. Definition and empirical characterization of creative processes. *Nonlinear Dyn Psychol Life Sci* 2003;7(1):35–47.
- [29] Sabelli H, Carlson-Sabelli L. Bios, a process approach to living system theory. In honour of James and Jessie Miller. *Syst Res Behav Sci* 2006;23(3):323–36.
- [30] Sabelli H, Messer J, Kovacevic L, Walthall K. The biotic pattern of heartbeat intervals. *Int J Cardiol* 2010;145(2):303–4.
- [31] Sabelli H, Sugerman A, Kovacevic L, Kauffman L, Carlson-Sabelli L, Patel M, et al. Bios data analyzer. *Nonlinear Dyn Psychol Life Sci* 2005;9(4):505–38.
- [32] Kauffman L, Sabelli H. Mathematical bios. *Kybernetes* 2002;31:1418–28.
- [33] Sadeghi G, Sheikhani A, Ashrafzadeh F. Poincare section analysis of the electroencephalogram in autism spectrum

- disorder using complement plots. *Kybernetes* 2017;46(2):364–82.
- [34] Goyette CH, Conners CK, Ulrich RF. Normative data on revised Conners parent and teacher rating scales. *J Abnorm Child Psychol* 1978;6(2):221–36.
- [35] Subha DP, Joseph PK, Acharya R, Lim CM. EEG signal analysis: a survey. *J Med Syst* 2010;34(2):195–212.
- [36] Pal PR, Khobragade P, Panda R. Expert system design for classification of brain waves and epileptic-seizure detection. *Students' Technology Symposium (TechSym)*, IEEE; 2011.
- [37] Rodriguez-Bermudez G, Garcia-Laencina PJ. Analysis of EEG signals using nonlinear dynamics and chaos: a review. *Appl Math Inf Sci* 2015;9(5):2309–21.
- [38] Chappell D, Panagiotidis T. Using the correlation dimension to detect non-linear dynamics: evidence from the Athens Stock Exchange. *EconWPA* 2005.
- [39] Roschke J, Fell J, Beckmann P. The calculation of the first positive Lyapunov exponent in sleep EEG data. *Electroencephalogr Clin Neurophysiol* 1993;86(5):348–52.
- [40] Pijn JP, Neerven JV, Noestc A, Silvad FHL. Chaos or noise in EEG signals; dependence on state and brain site. *Electroencephalogr Clin Neurophysiol* 1991;79(5):371–81.
- [41] Hilborn RC. Chaos and nonlinear dynamics: an introduction for scientists and engineers. Oxford University Press; 2000.
- [42] Wang Q, Sourina O, Nguyen MK. Fractal dimension based neurofeedback in serious games. *Vis Comput* 2011;27(4):299–309.
- [43] Yaghoobi R, Yaghoobi A. The effects of beta-I and fractal dimension neurofeedback on reaction time. *Int J Intell Syst Technol Appl* 2014;6(11):42–8.
- [44] Yaghoobi Karimui R, Azadi S. Cardiac arrhythmia classification using the phase space sorted by Poincare sections. *Biocybern Biomed Eng* 2017;37(4):690–700.
- [45] Lenartowicz A, Loo SK. Use of EEG to diagnose ADHD. *Curr Psychiatry Rep* 2014;16(11):1–11.
- [46] Williams LM, Hermens DF, Thein T, Clark CR, Cooper NJ, Clarke SD, et al. Using brain-based cognitive measures to support clinical decisions in ADHD. *Pediatr Neurol* 2010;42(2):118–26.
- [47] Loo SK, Cho A, Hale TS, McGough J, McCracken J, Smalley SL. Characterization of the theta to beta ratio in ADHD: identifying potential sources of heterogeneity. *J Atten Disord* 2013;17(5):384–92.
- [48] Liechti MD, Valko L, Müller UC, Döhnert M, Drechsler R, Steinhäusen HC, et al. Diagnostic value of resting electroencephalogram in attention-deficit/hyperactivity disorder across the lifespan. *Brain Topogr* 2013;26(1):135–51.
- [49] Buyck I, Wiersema JR. Resting electroencephalogram in attention deficit hyperactivity disorder: developmental course and diagnostic value. *Psychiatry Res* 2014;216(3):391–7.
- [50] Helgadóttir H, Guðmundsson ÓÓ, Baldursson G, Magnússon P, Blin N, Brynjólfssdóttir B, et al. Electroencephalography as a clinical tool for diagnosing and monitoring attention deficit hyperactivity disorder: a cross-sectional study. *BMJ Open* 2015;5(1):1–9.
- [51] Tenev A, Markovska-Simoska S, Kocarev L, Pop-Jordanov J, Müller A, Candrian G. Machine learning approach for classification of ADHD adults. *Int J Psychophysiol* 2014;93(1):162–6.
- [52] Ogrim G, Kropotov J, Hestad K. The quantitative EEG theta/beta ratio in attention deficit/hyperactivity disorder and normal controls: sensitivity, specificity, and behavioral correlates. *Psychiatry Res* 2012;198(3):482–8.
- [53] Sadatnezhad K, Boostani R, Ghanizadeh A. Classification of BMD and ADHD patients using their EEG signals. *Expert Syst Appl* 2011;38(3):1956–63.
- [54] Magee CA, Clarke AR, Barry RJ, McCarthy R, Selikowitz M. Examining the diagnostic utility of EEG power measures in children with attention deficit/hyperactivity disorder. *Clin Neurophysiol* 2005;116(5):1033–40.
- [55] Ahmadlou M, Adeli H. Wavelet-synchronization methodology: a new approach for EEG-based diagnosis of ADHD. *Clin EEG Neurosci* 2010;41:1–10.
- [56] Simoska S, Jordanova N. Quantitative EEG in children and adults with attention deficit hyperactivity disorder: comparison of absolute and relative power spectra and theta/beta ratio. *Clin EEG Neurosci* 2016;48(1):20–32.
- [57] Snyder SM, Quintana H, Sexson SB, Knott P, Haque AF, Reynolds DA. Multicenter validation of EEG and rating scales in identifying ADHD within a clinical sample. *Psychiatry Res* 2008;159(3):346–58.
- [58] Monastra VJ, Lubar JF, Michael L. The development of a quantitative electroencephalographic scanning process for attention deficit-hyperactivity disorder: reliability and validity studies. *Neuropsychology* 2001;15(1):136–44.
- [59] Mohammadi MR, Khaleghi A, Nasrabadi AM, Rafieivand S, Begol M, Zarafshan H. EEG classification of ADHD and normal children using non-linear features and neural network. *Biomed Eng Lett* 2016;6(2):66–73.
- [60] Abibullaev B, An J. Decision support algorithm for diagnosis of ADHD using electroencephalograms. *J Med Syst* 2012;36(4):2675–88.
- [61] Berger H. Über das elektroenzephalogramm des Menschen: Zweite Mittelung. *J Psychol Neurol (Lpz)* 1930;40:160–79.
- [62] Wrobel A. Beta activity: a carrier for visual attention. *Acta Neurobiol Exp (Warsz)* 2000;60(2):247–60.
- [63] Mundy-Castle AC. Theta and beta rhythm in the electroencephalograms of normal adults. *Electroencephalogr Clin Neurophysiol* 1951;3(4):477–86.
- [64] Clarke AR, Barry RJ, McCarthy R, Selikowitz M. EEG analysis in Attention-Deficit/Hyperactivity Disorder: a comparative study of two subtypes. *Psychiatry Res* 1998;81(1):19–29.
- [65] Lansbergen MM, Arns M, Dongen-Boomsma MV, Spronk D, Buitelaar JK. The increase in theta/beta ratio on resting-state EEG in boys with attention-deficit/hyperactivity disorder is mediated by slow alpha peak frequency. *Prog Neuropsychopharmacol Biol Psychiatry* 2011;35(1):47–52.
- [66] Koehler S, Lauer P, Schreppel T, Jacob C, Heine M, Boreatti-Hümmer A, et al. Increased EEG power density in alpha and theta bands in adult ADHD patients. *J Neural Transm* 2009;116(1):97–104.